CHAPTER 20

# PRESSURE-TEMPERATURE DIAGRAMS

When dealing with systems in which the gas phase must be considered, it is not generally satisfactory to limit observations to a fixed pressure as has been done in the presentation of temperature-composition diagrams. Pressure-temperature-composition (PTX) diagrams, such as those shown

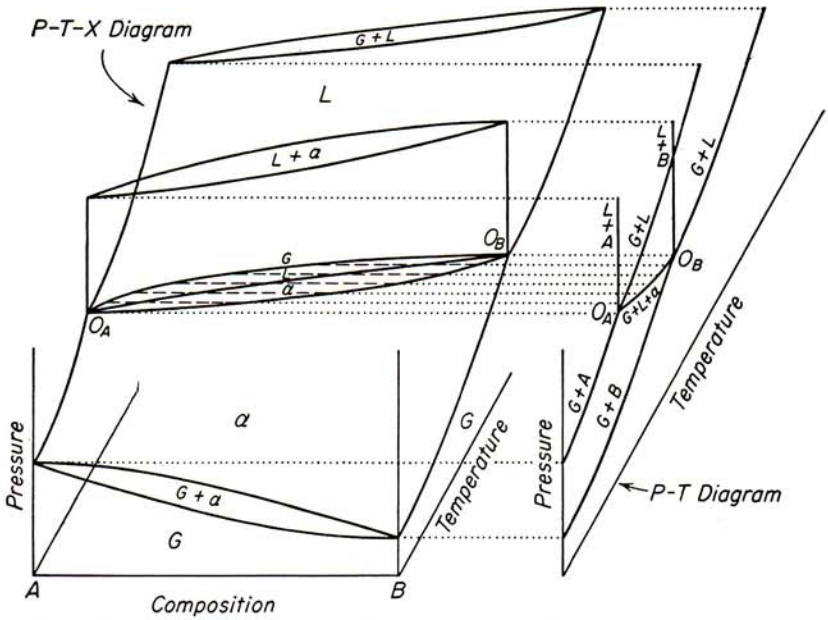


FIG. 20-1. PTX diagram of an isomorphous binary system showing how the PT diagram is derived by projecting all univariant and invariant equilibria upon the PT plane.

in Figs. 3-1 and 4-2, would be ideal for representing equilibria involving the gas phase were it not for the practical difficulty of handling three-dimensional diagrams. As an alternative it is often satisfactory to use pressure-temperature (PT) diagrams, in which the composition variable is ignored. These have the special advantage that they may be applied to systems of any number of components.

The PT diagram of a binary system can be derived from the PTX space diagram by projecting, upon a pressure-temperature plane, all points and lines representing invariant and univariant equilibrium in the space diagram (see Fig. 20-1). All lines from the one-component faces of the space

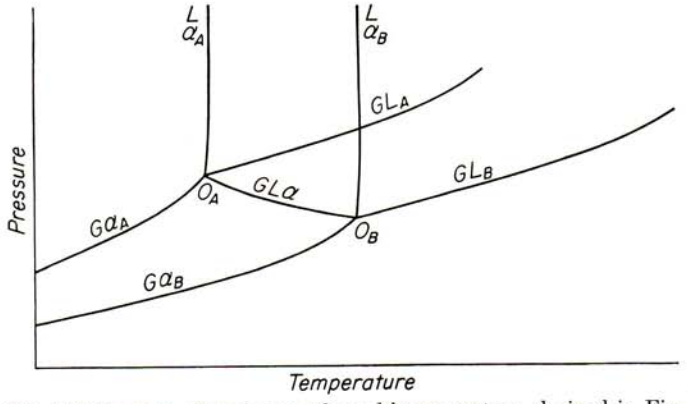


FIG. 20-2. PT diagram of an isomorphous binary system, derived in Fig. 20-1.

diagram are transferred directly to the PT projection, because these are univariant. From the inside, or binary, portion of the space diagram, only tie-lines that connect three or more conjugate phases are transferred to the PT diagram, three-phase equilibrium being univariant in binary systems. Since all tie-lines are both isobaric and isothermal, these project as

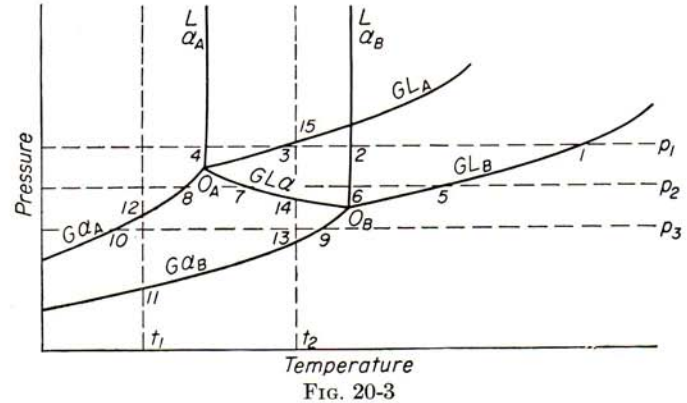


FIG. 20-3

points upon the PT plane. Any surface of the space figure that is generated by tie-lines therefore becomes a line in the PT diagram. In Fig. 20-1 there is a "ruled" surface, between points $O_A$ and $O_B$, composed of tie-lines connecting conjugate compositions of gas, liquid, and solid. This appears on the PT diagram as the line $G + L + \alpha$.

Displayed as normally drawn in two-dimensions, this PT diagram representing binary isomorphous equilibria appears in Fig. 20-2. Each line is labeled according to the equilibrium represented, the unary lines representing two-phase equilibrium and the binary line three-phase equilibrium. The areas between the lines cannot be identified uniquely, since the several bivariant and tervariant equilibria overlap one another in these areas. Invariant equilibrium occurs in this example only at the unary triple points $O_A$ and $O_B$.

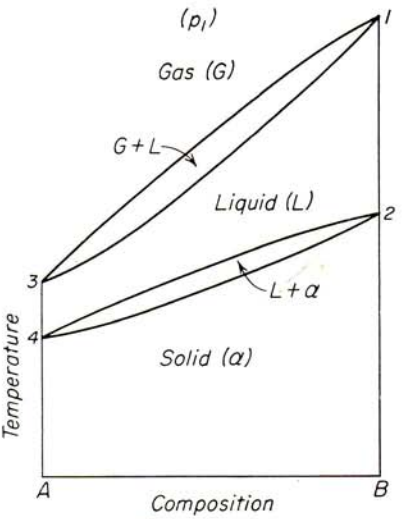


FIG. 20-4. Temperature-composition section at pressure $p_1$, derived from the PT diagram of Fig. 20-3.

This diagram may be employed to find the phase changes that occur during heating or cooling at any desired pressure or the phase changes that accompany pressure rise or fall at a stated temperature. The method used is illustrated in Fig. 20-3. Suppose that the pressure is fixed at $p_1$. Upon cooling from a very high tem-

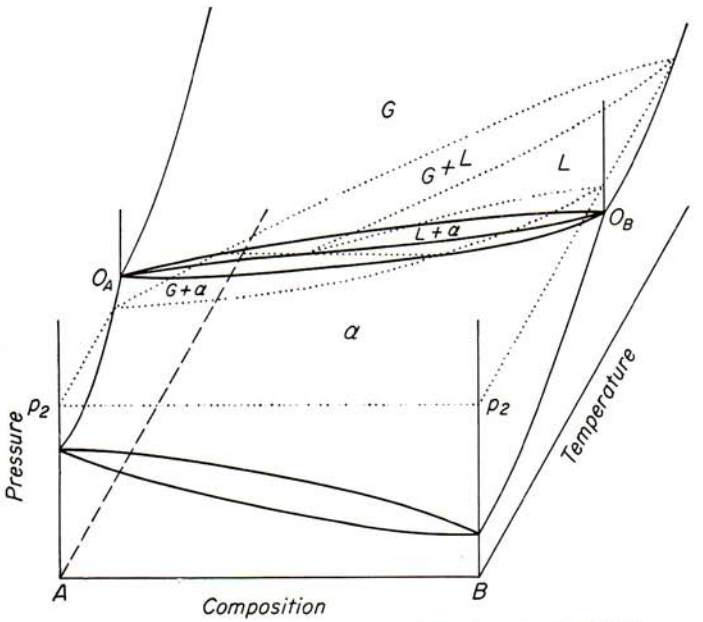


FIG. 20-5. Derivation of the TX section given in Fig. 20-7.

perature, component $B$ will begin to condense to liquid at the temperature of point 1; condensation of all compositions from $B$ to $A$ will occur between 1 and 3. At temperature 2 pure $B$ will begin to freeze, and mixtures of $A$ and $B$ will freeze between 2 and 4. Below the latter temperature all alloys are solid. This description is qualitatively the same as that

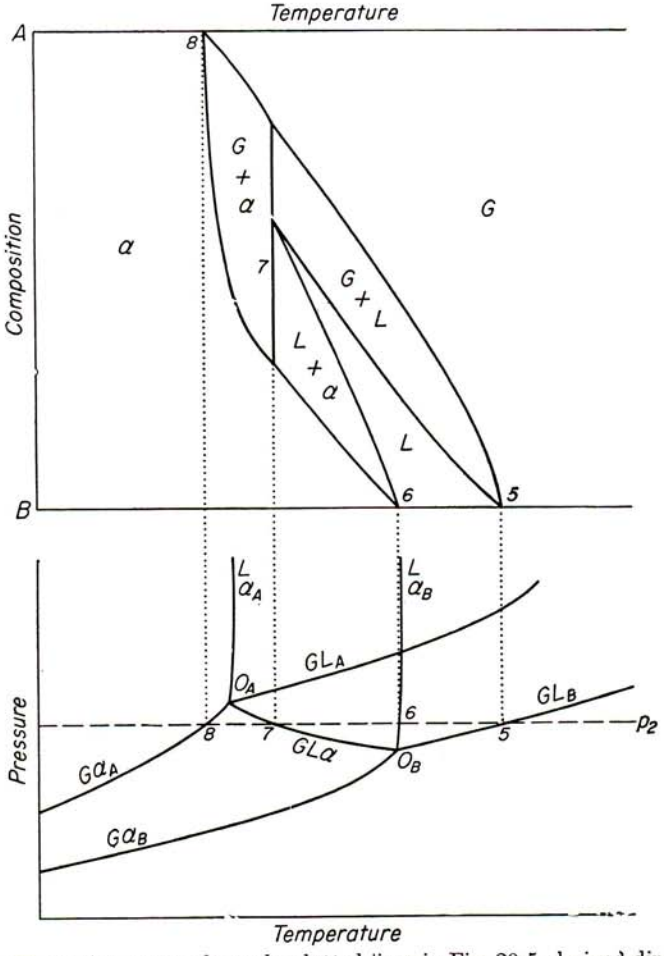


FIG. 20-6. TX section, at $p_2$, shown by dotted lines in Fig. 20-5, derived directly from the PT diagram by reading the temperatures of univariant equilibria where the dashed line $p_2$ intersects solid lines in the PT diagram.

presented by any binary TX diagram of an isomorphous system, such as that given in Fig. 20-4. Only a statement of the compositions of the conjugate liquid and solid phases at each temperature between 2 and 4 and of the conjugate gas and liquid phases between 1 and 3 is lacking.

At a lower pressure $p_2$, Fig. 20-3, the univariant equilibrium among gas, liquid, and $\alpha$ is encountered. Condensation of the vapor phase begins at the temperature of point 5 where pure $B$ condenses to its liquid. From 5 to 7 the condensation of alloys of increasing $A$ content begins. Pure $B$ freezes at the temperature of point 6, and alloys of advancing $A$ content begin to freeze at progressively lower temperatures down to 7. In alloys of intermediate composition the liquid phase decomposes ($L \rightarrow G + \alpha$) at temperature 7. Below this temperature only solid and vapor can exist at this pressure. The gas now condenses directly to the solid phase at temperatures that decrease to 8 as the composition approaches pure $A$.

These relationships will be more easily perceived in the TX section drawn at pressure $p_2$, Fig. 20-7. Its derivation from the PTX diagram is demonstrated in Fig. 20-5, and its derivation from the PT diagram in

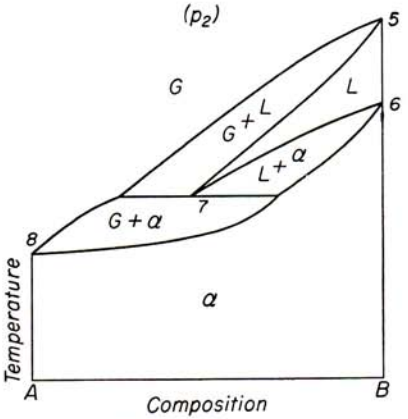


FIG. 20-7. TX section at $p_2$, derived from Figs. 20-3, 20-5 and 20-6.

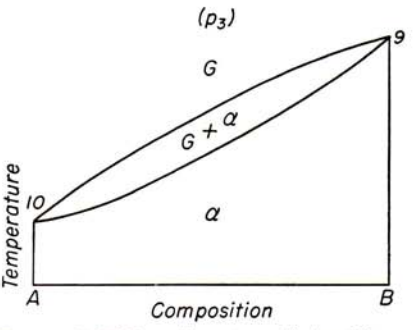


FIG. 20-8. TX section at $p_3$, derived from the PT diagram of Fig. 20-3.

Fig. 20-6. Each line in the PT diagram, Fig. 20-6, intersected by the horizontal line $p_2$ designates the temperature of a univariant equilibrium in the TX diagram. The composition at which each univariant equilibrium should be recorded in the TX diagram is inferred from the labeling of the lines in the PT diagram. All two-phase equilibria are unary and so are plotted at the extreme right or left of the TX diagram, points 5, 6, and 8. Three-phase equilibria are binary and must be represented by a single three-phase tie-line, point 7 in the PT diagram and line 7 in the TX diagram. Three points on the horizontal line arbitrarily chosen to designate the compositions of the three conjugate phases $G$, $L$, and $\alpha$ are connected to corresponding unary points to complete the TX diagram. In Fig. 20-7 it will be observed that the liquid phase undergoes a eutectic type of transformation, in which gas and one solid phase are produced simultaneously (see Table 2, case *e*). In most isomorphous alloys this reaction

would occur at such low pressure that it could not be realized except at the surface of the metal, even in the highest vacuum. This is because the hydrostatic head of metal would exceed $p_2$ except at the extreme surface. By this type of reaction, however, the surface of the alloy, frozen in vacuum, would become depleted with respect to the more volatile component $A$. Some other types of systems in which this kind of reaction occurs at higher pressure will be discussed presently. Where surface behavior is of interest, of course, such low pressure transformations become significant.

At still lower pressure, $p_3$ in Fig. 20-3, the liquid phase is missed altogether and alloys of any composition, upon equilibrium heating, sublime directly to the vapor phase or, upon equilibrium cooling, condense directly to the solid phase (see Fig. 20-8). Again, such effects, upon heating, are likely to be confined to the extreme surfaces of pieces of metal, where the low pressure can be attained. Condensation from the vapor phase produces very minor quantities of solid metal at the very low pressures at which such effects usually occur. All such effects are perceptible, however, under special conditions.

Two particularly interesting characteristics of the PT diagram are revealed in the foregoing discussion. First, the general form of the PT diagram can be established upon the basis of a very few facts concerning the alloy system. In this case, it is necessary to know only the approximate coordinates of the triple points of $A$ and $B$ and that the system is isomorphous, without complications. Nothing more is needed for a qualitatively correct representation, although the exact location of each of the curves would require lengthy and often very difficult laboratory investigation. The second characteristic of special interest is that the form of the TX diagram for any given pressure can be derived directly from the PT diagram. Compositions of phases cannot be ascertained from the PT diagram, of course, but the several phases will occur upon the derived TX diagram in the correct composition sequence. Thus, a TX diagram is obtained which is capable of answering many practical questions and, also, one which can be made roughly quantitative with a very few additional data, such as measurement of the exact temperatures of univariant reaction together with determination of the compositions of the three conjugate phases involved in each reaction.

### Pressure-Composition (PX) Diagrams

Two isothermal sections are indicated in Fig. 20-3 by the vertical dashed lines designated $t_1$ and $t_2$. Pressure-composition (PX) diagrams may be derived in the same way that the TX diagrams are derived, namely, by plotting the (numbered) intersections of the isothermal lines

and the univariant curves of the PT diagram upon the coordinates of a PX diagram and connecting these points in the only way possible with boundaries of divariant fields (see Figs. 20-9 and 20-10). The resulting PX diagrams are very similar to the corresponding TX diagrams, with reversal of the relative positions of the several fields. Metallurgical uses of PX diagrams are rare, because conditions involving constant temperature and variable pressure are infrequently encountered. The construction

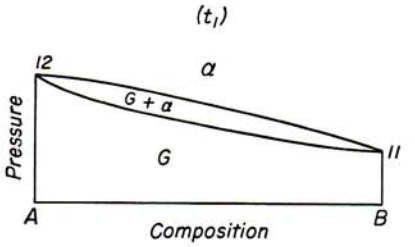


FIG. 20-9. PX section at $t_1$, derived from the PT diagram of Fig. 20-3.

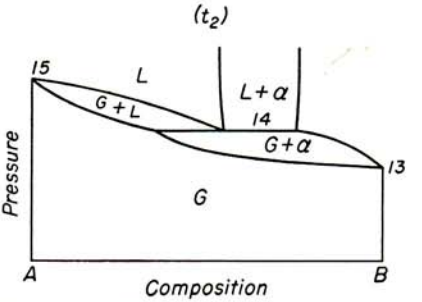


FIG. 20-10. PX section at $t_2$, derived from the PT diagram of Fig. 20-3.

and interpretation of the appropriate PX diagrams parallel so closely those of the TX diagrams, which have formed the principal subject of this book, that no special discussion of the matter is required.

## Invariant Equilibrium in Binary Systems

The PT diagram of a binary eutectic system, corresponding to the PTX diagram shown in Fig. 4-2, is given in Fig. 20-11. As in the previous example, three triple curves of each of the components are indicated, joining at the two triple points $O_A$ and $O_B$. There are, in addition, four binary univariant curves, or *quadruple curves*, $L\alpha\beta$, $G\alpha\beta$, $GL\alpha$, and $GL\beta$, that meet at a *quadruple point* $Q$. This point represents invariant equilibrium among the four phases $G$, $L$, $\alpha$, and $\beta$; its pressure and temperature coordinates are fixed, and the compositions of each of the four conjugate phases are also fixed.

Every quadruple point is associated with four quadruple curves each of which represents equilibrium among a unique combination of three of the four phases occurring at invariant equilibrium. The quadruple curve representing equilibrium among liquid and two solid phases (the eutectic reaction) usually projects almost vertically upward (Fig. 20-11). A slight tilt toward higher temperature with increasing pressure is normal when both components contract upon freezing. The $G\alpha\beta$ curve always proceeds to lower temperature with falling pressure, frequently at a slope such that

it would end at zero pressure and the absolute zero of temperature. This curve always lies above both of the unary sublimation curves in eutectic systems, because it represents the total vapor pressure of the two solid phases coexisting. Two quadruple curves $GL\alpha$ and $GL\beta$ connect the quadruple point with the two triple points $O_A$ and $O_B$. One of these proceeds

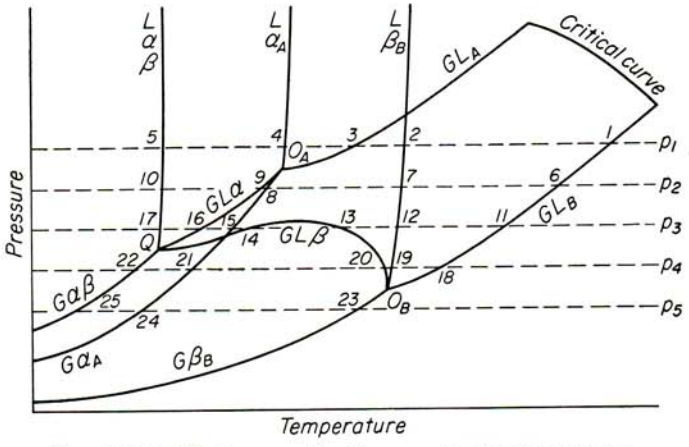


FIG. 20-11. PT diagram of a binary eutectic-type system.

continuously upward from the quadruple point $Q$ to the higher of the two triple points $O_A$.[1] The other of these curves may, and frequently does, pass through a pressure maximum between the quadruple point and the lower triple point $O_B$ (see Fig. 20-11).

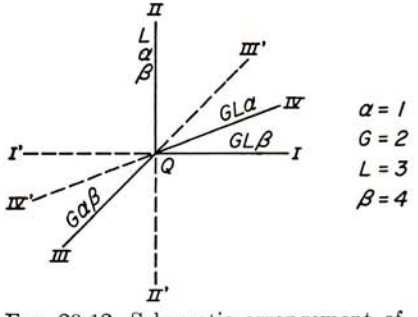


FIG. 20-12. Schematic arrangement of the quadruple curves about the quadruple point $Q$ in Fig. 20-11.

There is a thermodynamic rule that relates the succession of the quadruple curves about the quadruple point with the relative concentrations of the four phases. First, the phases are numbered 1, 2, 3, and 4 in their order of ascending or descending $B$ content; in Fig. 4-2 this order would be $\alpha = 1$, $G = 2$, $L = 3$ and $\beta = 4$. Then the quadruple curves are numbered I, II, III, and IV, using the numeral I to designate that equilibrium from which the first phase is missing, and so on. The quadruple curves, so numbered, should occur clockwise or counterclockwise in the

[1] An exception to this rule occurs when the quadruple point occurs at a pressure maximum. This special case is relatively uncommon and will not be discussed here. For details, see R. Vogel, "Handbuch der Metallphysik," II. Die Heterogenen Gleichgewichte, pp. 199–200, Akademische Verlagsgesellschaft m.b.h., Leipzig, 1937.

following order: I, II′ (i.e., extension of II), III, IV′ (i.e., extension of IV), I′ (i.e., extension of I), II, III′ (i.e., extension of III), and IV (see Fig. 20-12). This rule excludes the possibility of any adjacent quadruple curves meeting at an angle in excess of 180°. By reversing the above computation, the order of compositions of the four conjugate phases represented at any quadruple point as shown on a PT diagram can be ascertained.

Examples of five different configurations of the TX sections, taken at pressure $p_1$ to $p_5$, Fig. 20-11, appear in Figs. 20-13 to 20-17 inclusive. The first of these, corresponding to $p_1$, is the familiar simple eutectic diagram.

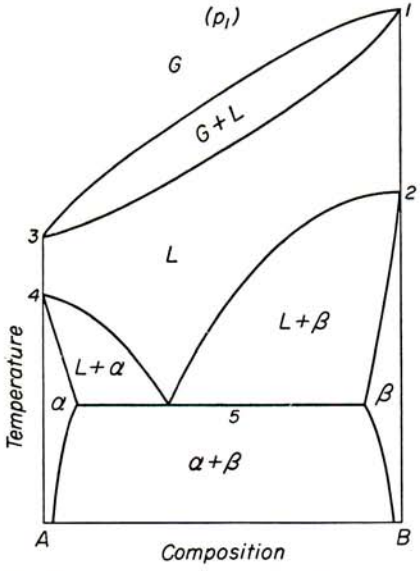


FIG. 20-13. TX section at $p_1$, derived from the PT diagram of Fig. 20-11.

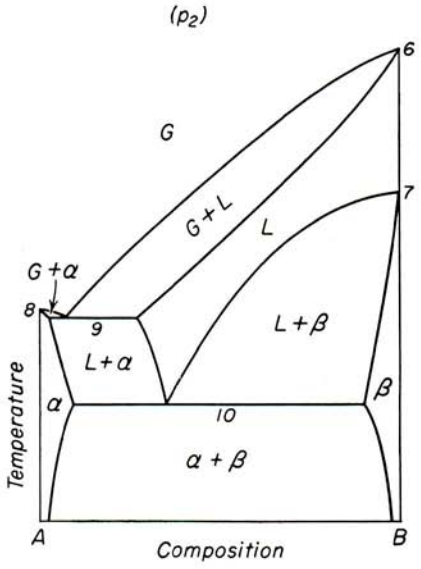


FIG. 20-14. TX section at $p_2$, derived from the PT diagram of Fig. 20-11.

Below the triple point of component $A$, at $P_2$, the liquid phase is confined to $B$-rich alloys, while the $A$-rich alloys cannot be fully melted under equilibrium conditions because sublimation intervenes (Fig. 20-14).

At somewhat lower pressure, $p_3$, the same horizontal line intersects the $GL\beta$ quadruple curve in two places, below its maximum. This gives rise to a double occurrence of the equilibrium $GL\beta$ in the TX diagram (see Fig. 20-15). Accordingly, alloys rich in the $B$ component exhibit double melting and double boiling. Melting first occurs at the equilibrium $L\alpha\beta$ (line 17); this liquid "boils," or actually decomposes into gas and $\beta$, at the lower $GL\beta$ line (line 14). Again, at the upper $GL\beta$ equilibrium (line 13) liquid appears (melting) and finally boils away, incongruently, to vapor. An easily visualized example of this case is found in salt-water mixtures,

which are composed of ice and crystalline salt at low temperature, of water and crystalline salt at room temperature, of steam and crystalline salt above the "boiling point," of molten salt at very high temperature, and of vapor alone at extremely high temperature. Similar conditions are to be expected in metal-hydrogen systems where no hydride forms. Let $A$ represent hydrogen and $B$ the metal; the upper liquid field (Fig. 20-15) would represent the molten metal with dissolved hydrogen, and the lower liquid field, which would occur only at very low temperature and close to the "$A$ side" of the diagram, would represent liquid hydrogen. If molten metal containing dissolved hydrogen were cooled, the primary freezing process would end with an evolution of gas which would probably be nearly pure hydrogen because the $GL\beta$ line would extend almost across the diagram. Remelting at lower temperature would not be observed, because room temperature occurs far above the lower boiling point in this case.

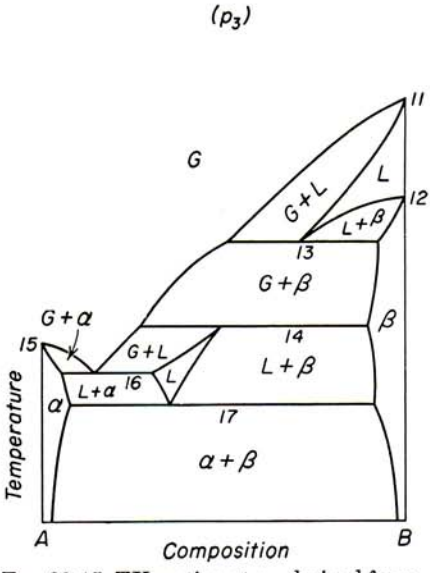


FIG. 20-15. TX section at $p_3$, derived from the PT diagram of Fig. 20-11.

Somewhat similar conditions are found in the TX section at $p_4$, Fig. 20-16, below the quadruple point. No low-temperature occurrence of the

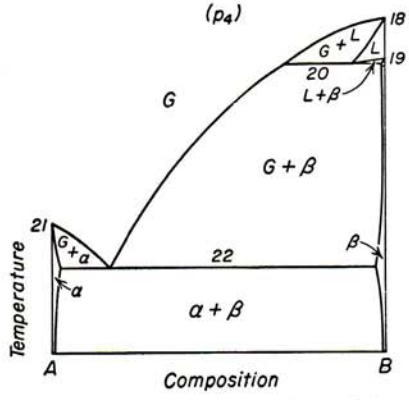


FIG. 20-16. TX section at $p_4$, derived from the PT diagram of Fig. 20-11.

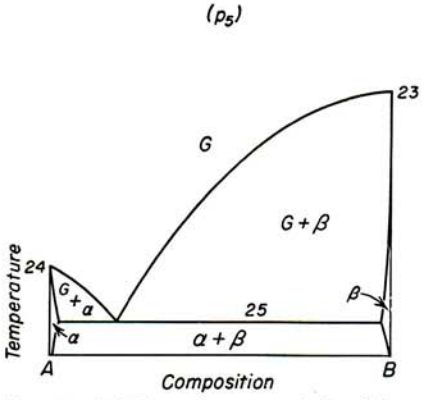


FIG. 20-17. TX section at $p_5$, derived from the PT diagram of Fig. 20-11.

liquid phase is found, however, at this low pressure. Alloys rich in $B$ would exhibit gas evolution during freezing, as at higher pressure. Finally, at very low pressure, $p_5$, Fig. 20-17, the liquid phase is entirely absent from "equilibrium transformation." Upon cooling, the gas phase itself deposits a two-phase alloy of $\alpha + \beta$. This type of reaction is usually confined to such low pressure in metal systems that familiar examples are lacking, although a closely related behavior is found in the operation of arsenic kitchens when oxides of impurity metals condense with the arsenic.

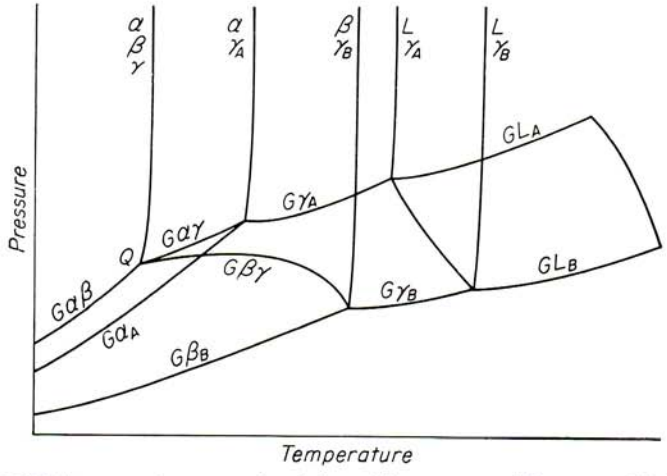


FIG. 20-18. PT diagram of a system involving a binary eutectoid-type equilibrium at $Q$.

By changing the pressure and temperature relationships on the PT diagram, some other configurations of the TX diagram are obtained. However, the previously cited examples include all cases that are well known in metal systems, and since, furthermore, the other TX sections are readily derived, there is little to be gained by exhausting the subject here.

### Some Other Binary Quadruple Points

All quadruple points associated with high-pressure equilibria of the eutectic class, i.e., eutectoids, monotectics, have the arrangement of quadruple curves illustrated in Fig. 20-12, namely, one "vertical" curve, one proceeding toward lower temperature, and two toward higher temperature. An example of a PT diagram from which the simple eutectoid diagram of Fig. 5-1 may be derived is given in Fig. 20-18. Here the quadruple point $Q$ represents equilibrium among gas, $\alpha$, $\beta$, and $\gamma$. It will be evident that an analysis of the low-pressure behavior of this system will lead to the conclusion that the decomposition of the $\gamma$ phase, like that of

the liquid phase in the previous example, can be accompanied by gas evolution.

The monotectic system, illustrated in Fig. 6-1, may be derived from the PT diagram of Fig. 20-19. Two quadruple points appear in this diagram, $Q_1$ corresponding to eutectic reaction at low temperature and $Q_2$ to

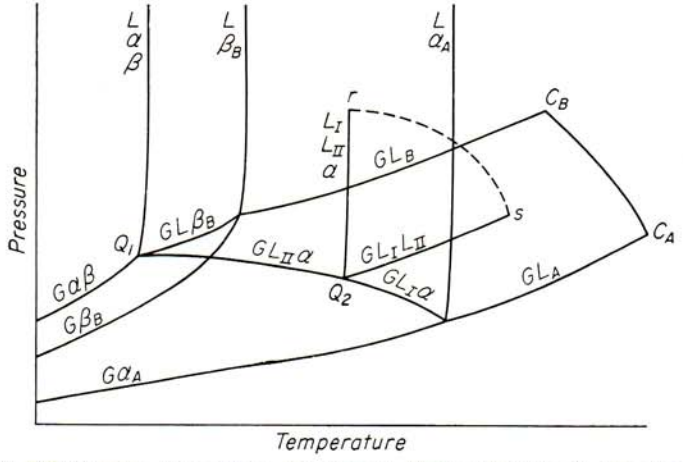


FIG. 20-19. PT diagram of a system involving a binary monotectic-type equilibrium at $Q_2$.

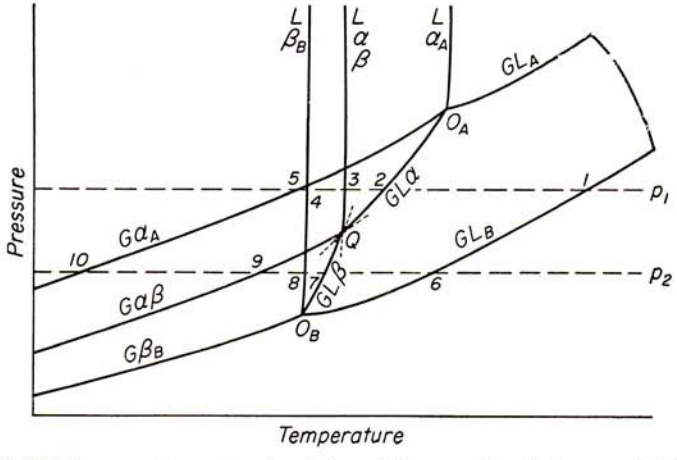


FIG. 20-20. PT diagram of a system involving a binary peritectic type equilibrium at $Q$.

monotectic reaction at higher temperature. Three phases, gas, liquid II, and $\alpha$, are common to the two quadruple points, and the quadruple curve representing equilibrium among these three phases serves to connect the quadruple points. The $GL_IL_{II}$ curve is shown ending in a critical point at $s$; other configurations are possible. In like manner the $L_IL_{II}\alpha$

curve is shown terminating upon a critical point at $r$. When this happens the field of $L_I + L_{II}$ has a critical curve following the path of the dashed line $rs$.

With peritectic reaction, as in Fig. 8-1, the disposition of the quadruple curves is reversed: one is "vertical," two proceed toward lower tempera-

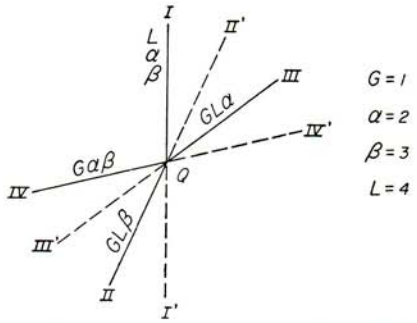


FIG. 20-21. Schematic representation of the arrangement of the quadruple curves about the quadruple point $Q$ in Fig. 20-20.

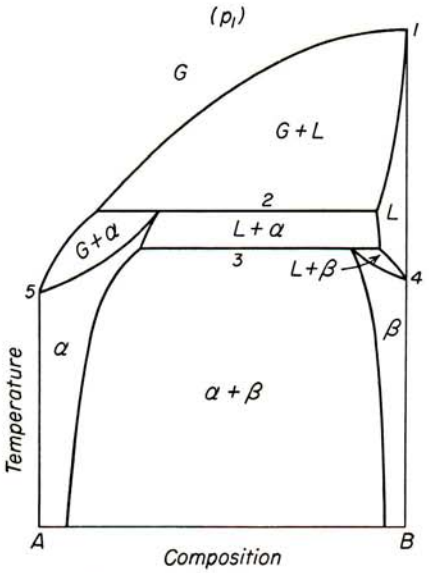


FIG. 20-22. TX section at $p_1$, derived from the PT diagram of Fig. 20-20.

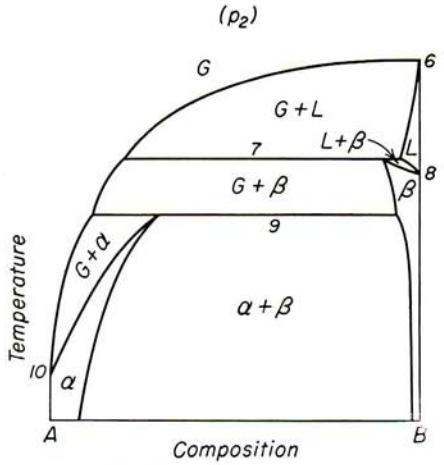


FIG. 20-23. TX section at $p_2$, derived from the PT diagram of Fig. 20-20.

ture, and only one toward higher temperature (see Fig. 20-20). The application of the rule of succession of quadruple curves is illustrated for the peritectic case in Fig. 20-21. All three-phase equilibria of the peritectic class, such as peritectoids and syntectics, originate upon quadruple points of the same form. Two low-pressure configurations of the TX dia-

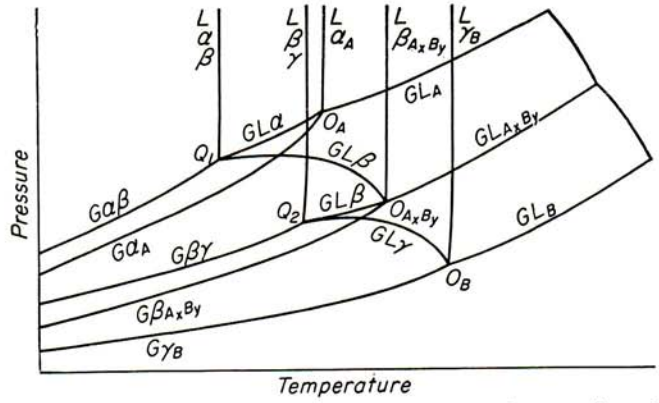


FIG. 20-24. PT diagram of a system having a fully congruent intermediate phase $AxBy$.

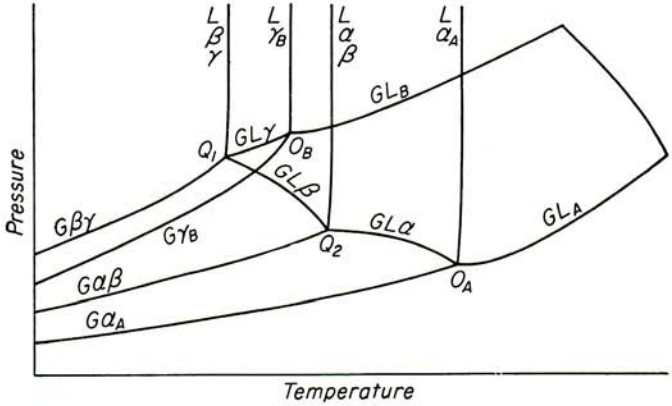


FIG. 20-25. PT diagram of a system having a peritectic-type binary equilibrium $Q_2$ and a eutectic-type binary equilibrium $Q_1$.

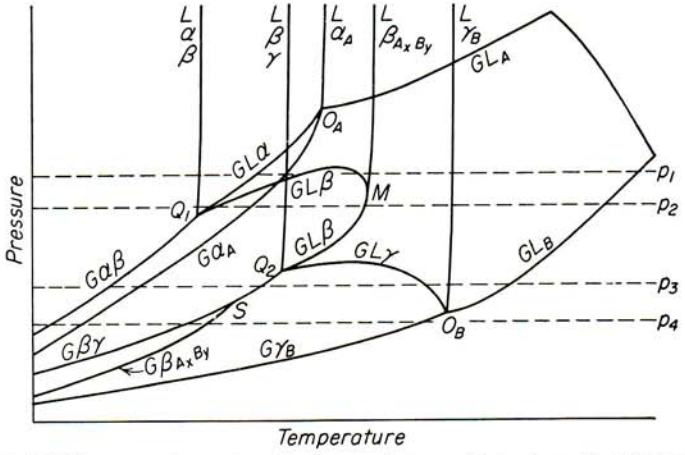


FIG. 20-26. PT diagram of a system having an intermediate phase that is incongruent in the pressure-temperature range from the maximum sublimation point $S$ to the minimum melting point $M$.

gram, characteristic of this type of system, are shown in Figs. 20-22 and 20-23. The "peritectic" decomposition of a solid phase into gas and liquid appears in both of these TX sections. A reaction similar to the upper three-phase equilibrium in Fig. 20-23 is thought to occur in the palladium-hydrogen system where the palladium-rich solid phase melts with evolution of gas.

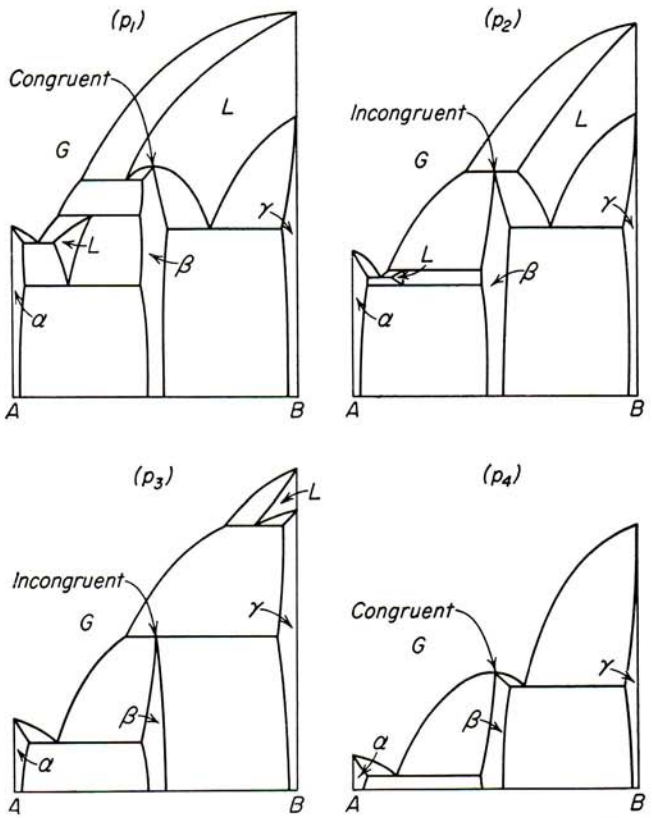


FIG. 20-27. Temperature-concentration sections derived from the PT diagram of Fig. 20-26.

Intermediate phases may be congruent throughout the entire range of pressure and temperature, having their own triple points and triple curves as shown in Fig. 20-24; they may be incongruent in all ranges as is the $\beta$ phase of Fig. 20-25 (Fig. 8-2 is derived from this PT diagram); or the intermediate phase may be congruent in some ranges and incongruent in others. The latter case, as illustrated in Fig. 20-26, is thought to occur in several metal-oxygen systems, notably copper-oxygen. Instead of having a triple point, the intermediate phase is congruent only above a certain

minimum pressure, the minimum melting point $M$. Below this pressure it melts with decomposition and sublimes, also with decomposition, down to the pressure of the maximum sublimation point $S$, below which congruent sublimation is observed. These conditions are demonstrated in the isobaric sections of Fig. 20-27, taken at the four pressure levels indicated in Fig. 20-26. The maximum sublimation point may occur anywhere upon the curve $G\beta\gamma$ or anywhere below $M$ on the curve $GL\beta$.

## Ternary and Higher-Order PT Diagrams

Since the concentration variable is not represented in PT diagrams, there is fundamentally no limit to the number of components that may be handled. Actually, the diagrams become extraordinarily intricate, and

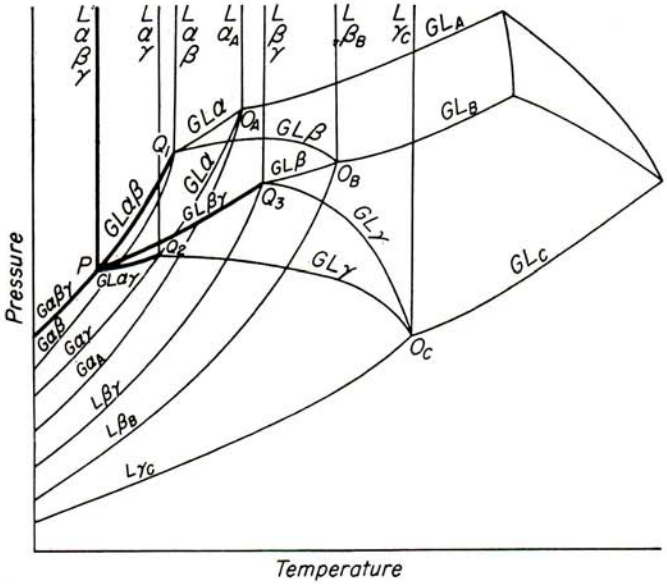


FIG. 20-28. PT diagram of a ternary eutectic-type (class I) system.

therefore difficult to read, as the number of components is increased. Even a simple ternary eutectic system (Fig. 20-28) is relatively complex in its representation. In this example there are three triple points and sets of triple curves, corresponding to the three components, three binary (eutectic) quadruple points and accompanying quadruple curves, and one ternary quintuple point $P$ from which issue five quintuple curves, three of which connect the quintuple point with the three quadruple points. All three of these quintuple curves proceed from the quintuple point to higher temperature, while one curve ($G\alpha\beta\gamma$) goes to lower temperature.

This is characteristic of all class I ternary equilibria (Fig. 20-29*a* and recall Fig. 18-1*i*). Quintuple points representing class II equilibrium have two curves running toward higher temperature and two toward lower temperature (Fig. 20-29*b*), while class III (Fig. 20-29*c*) equilibrium is the reverse of class I (recall Fig. 18-1*i*, *j*, and *k*).

Complex PT diagrams are read in the same manner as are the binary types. It is not difficult to derive ternary temperature-concentration diagrams as can be seen by comparing Fig. 20-28, at high pressure, with Fig. 14-1, to which it corresponds.

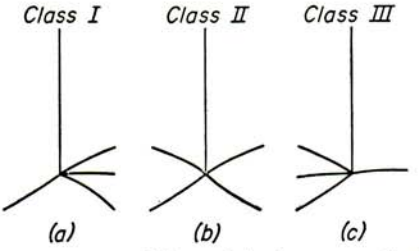


FIG. 20-29. Schematic arrangement of the quintuple curves about the quintuple point (such as *P* in Fig. 20-28) for the three classes of ternary univariant equilibrium.

It will be evident that higher-order systems will involve increasing numbers of phases in their univariant and invariant equilibria. Quaternary systems will have four kinds of sextuple points each with six sextuple curves, quinary systems five kinds of septuple points with seven radiating septuple curves, and so on. No complex metal systems are known to have been investigated with regard to their pressure-temperature equilibria, and no diagrams are available.